IUST
Iran University of
Science and Technology

Iranian Journal of Electrical and Electronic Engineering

Journal Homepage: ijeee.iust.ac.ir

Exploring the Potential of Cloud Fertilization through Electromagnetic Wave Scattering Analysis

Aslan Nouri Moqadam*, Seyed Hosein Mousavi*(C.A.)

Abstract: Electromagnetic waves, with their unique properties, offer promising solutions to environmental challenges. This paper explores the utilization of electromagnetic scattering by droplets for cloud fertilization purposes. Specifically, a linearly polarized plane wave is deployed to stimulate a heterogeneous cloud medium composed of spherical droplets with varying size parameters. Through the application of Generalized Mie Theory (GMT) and Discrete Dipole Approximation (DDA) at a frequency of 28 GHz, multiple scattering phenomena and local electric fields are meticulously computed. Various scenarios of scattering, encompassing droplet diameters ranging from 500 µm to 700 µm and diverse volume fractions, are meticulously examined. Employing DDA and dyadic calculations, the exerted forces on individual spherical droplets are rigorously evaluated, with precise determination of force direction and components. The droplet density influences the RCS values, with a maximum of -15 dBm2 in the case of varying droplet distribution. According to the simulation, an exerted force reached up to the absolute value of 72.98 (µN) for randomly distributed droplets. The simulations robustly affirm the viability of droplet manipulation via plane wave excitation, thereby enhancing the likelihood of droplet collision and consequent cloud fertilization, ultimately leading to precipitation. Furthermore, the parameters of the incident wave can be deliberately adjusted to steer droplets toward denser regions, thereby augmenting the likelihood of successful fertilization events.

Keywords: Droplet, Electromagnetic Scattering, Fertilization, Polarization.

1 Introduction

RECENTLY, there has been notable scientific interest in the electromagnetic (EM) waves and their characteristics regarding environmental challenges. Issues such as air pollution and drought present significant challenges, which EM waves have shown potential to address. Applications include intentionally redirecting dust particles to mitigate air pollution and stimulating cloud formation to combat drought. Detailed investigation into EM waves and their interactions with the surrounding medium is warranted. Harnessing EM waves effectively can yield remarkable benefits for human life across various applications. It is imperative to evaluate the behavior of these waves in different propagation mediums, considering factors such as temperature, rain rate, and frequency. Numerous studies have examined how rain and climate variations affect EM wave propagation properties, highlighting their sensitivity to environmental parameters [1-2]. The quality of communication systems is greatly influenced by attenuation experienced by EM waves in propagation mediums. Previous research has delved into factors such as realistic raindrop shapes [3] and frequency [4] effects to comprehensively understand propagation characteristics in rainy conditions. Additionally, studies have explored the behavior of EM waves in environments containing dust particles, deriving expressions for attenuation and phase shift coefficients in mediums with sand and dust [5].

To attain a thorough understanding of the behavior of EM waves in heterogeneous media which can be the

Iranian Journal of Electrical & Electronic Engineering, 2025.
Paper first received 19 August 2024 and accepted 24 November 2024.
* The authors are with the Faculty of Electrical and Computer Engineering, University of Tabriz, Tabriz, Iran.
E-mail: mir.hosein.mousavi@tabrizu.ac.ir.
Corresponding Author: Seyed Hosein Mousavi.

human body [6], it is essential to thoroughly examine the scattering phenomenon of EM waves. When EM waves encounter discontinuities or propagate through anisotropic mediums, they deviate from their initial trajectory [7]. This phenomenon, known as scattering, involves the atomic rearrangement of positive and negative charges in response to the EM wave, resulting in oscillation [8]. This atomic oscillation tends to emit radiation, causing the primary wave to transform into multiple waves propagating along different paths.

Various methodologies have been utilized to examine the phenomenon of multiple scattering by particles of arbitrary shapes. The Mie Theory, which describes scattering by a single homogeneous sphere whose size is comparable to the wavelength, serves as the fundamental theory for spherical particles [8]. In the late 20th century, the study of electromagnetic scattering by aggregates of spheres was extended through the use of the Generalized Multi-particle Mie Theory (GMMT), applicable to variously shaped small particles [9-10]. Transition Matrix techniques offer expressions for scattering by random shapes such as finite cylinders and spheres, initially derived for ensembles of spheres by Mackowski [11]. Additionally, methods such as Rayleigh scattering and the discrete dipole approximation (DDA) have been employed to investigate multiple scattering from small particles compared to the wavelength [12].

When considering clouds as dense random media comprised of spherical drops interacting with EM waves, a comprehensive evaluation of the electromagnetic radiation's behavior and impact can be conducted. EM radiation, along with the pressure and force exerted on the drops, can agitate and align them within the cloud. This phenomenon can result in the generation of electric charge, potentially leading to cloud fertilization and intentional rainfall. By regarding the drops as spheres with radii much smaller than the illuminating wavelength, the electric force and its direction can be calculated using Lorentz's theorem [13-14].

Additionally, [15] examines the effect of droplet shape and deformation on the multiple scattering of incident waves, providing equations and relations for spherical, elliptical and oblate droplet shapes. In [15], the scattering of EM waves is analyzed without addressing the exerted force on droplets. Also, [16] discussed rain attenuation and statistical distribution of raindrop sizes at a frequency of 38 GHz, and [17] investigates droplet shape deformation due to polarization effects from multi-polarization radar, while it lacks analysis on exerted forces and multiple scattering, focusing instead on single-droplet deformation.

This study investigates several scenarios involving random media composed of spherical raindrops to assess multiple scattering phenomena and compute the exerted Lorentz force on the drops. By leveraging the exerted force on the drops, the direction of force from an incident plane wave can be estimated. In this paper, how EM waves can be used to influence particle movement has been explored, specifically cloud droplets, under conditions unfavorable for rainfall, such as low wind and uncharged droplets. The use of EM waves in environmental applications holds significant promise. By deliberately directing cloud droplets, facilitating their convergence, potentially inducing electrical charging and cloud seeding. Various mediums comprising 10 and 15 spherical particles with diameters ranging from 500 to 700 micrometers are examined to determine the precise magnitude and direction of the Lorentz force. According to [1] rain droplet sizes range from 0.25 to 4 mm, while drizzle droplets average between 0.2 and 0.5 mm. this range was chosen arbitrarily, based on the available data on droplet sizes. Through several simulations, the feasibility of cloud fertilization using EM waves is confirmed. The GMMT and DDA methods are employed to assess EM wave scattering in the anisotropic medium, and the resulting force magnitude and direction are documented.

The structure of this paper is as follows: Section 2 outlines the problem statement and models the inhomogeneous medium. Section 3 evaluates the techniques utilized for assessing multiple scattering and determining the Lorentz force. Section 4 discusses the results under different conditions regarding the exerted force to validate the feasibility of cloud fertilization using EM waves. Finally, Section 5 concludes by summarizing the methods and results, underscoring the reliability of employing EM waves for intentional cloud fertilization.

2 Statement of the Problem

This paper considers the cloud medium as comprising a cluster of small spherical particles distributed randomly. Each sphere is defined by its radius a^l and electrical permittivity ε^l, where $l = 1.2 \ldots . n$. The paper employs the Lorentz force method to calculate the direction and magnitude of force exerted on each spherical particle. The deliberate deviation of particles to intersect each other results in the rubbing of cloud drops, facilitating fertilization. Subsequent sections will delve into the theoretical framework of random scattering and the determination of Lorentz force on arbitrarily oriented cloud drops.

In the Cartesian coordinate system centered at the sphere's origin, the incident wave on each sphere consists of both the main excitation wave and the wave scattered by other spheres. Vector spherical wave functions (VSWF) are utilized to expand the scattered,

internal, and incident EM fields [7]:

$$E_{inc}^{l} = -E_0 \sum_{n=1}^{\infty} \sum_{m=-n}^{n} i^{n+1} \left[p_{mn}^{l} \bar{N}_{mn}^{(1)l} + q_{mn}^{l} \bar{M}_{mn}^{(1)l} \right] \quad (1)$$

$$E_{sca}^{l} = E_0 \sum_{n=1}^{\infty} \sum_{m=-n}^{n} i^{n+1} \left[a_{mn}^{l} \bar{N}_{mn}^{(3)l} + b_{mn}^{l} \bar{M}_{mn}^{(3)l} \right] \quad (2)$$

$$E_{\text{int}}^{l} = -E_0 \sum_{n=1}^{\infty} \sum_{m=-n}^{n} i^{n+1} \left[d_{mn}^{l} \bar{N}_{mn}^{(1)l,\text{int}} + c_{mn}^{l} \bar{M}_{mn}^{(1)l,\text{int}} \right] \quad (3)$$

where:

$$\bar{M}_{mn}^{(l)} = \left[\hat{e}_\theta i\pi_{mn}(\theta) - \hat{e}_\varphi \tau_{mn}(\theta) \right] z_n^{(l)}(\rho) \times \exp(im\varphi) \quad (4)$$

$$\bar{N}_{mn}^{(l)} = \{ \hat{e}_r n(n+1) P_n^m(cos\,\theta) \frac{z_n^{(l)}(\rho)}{\rho} + [\hat{e}_\theta \tau_{mn}(\theta) + \hat{e}_\varphi i\pi_{mn}(\theta)][\rho z_n^{(l)}(\rho)]/\rho \} \times \exp(im\varphi) \quad (5)$$

Without loss of generality, this paper considers an incident EM plane wave propagating in the positive z-direction, with linear polarization defined by an angle β_p. This wave illuminates the multi-sphere system. For the mentioned type of incident wave, the expansion coefficients take on a simple form:

$$q_{mn}^{l} = -\exp(ikZ^l)\, m\delta_{|m|,1} \frac{\sqrt{2n+1}}{2} \exp(-im\beta_p) \quad (6)$$

$$p_{mn}^{l} = \exp(ikZ^l)\, m\delta_{|m|,1} \frac{\sqrt{2n+1}}{2} \exp(-im\beta_p) \quad (7)$$

At the surface of a dielectric sphere, as there are no magnetic or electric charges present, the internal and external EM fields should cancel each other out. Therefore, the boundary condition at the surface is as demonstrated below:

$$(E^i + E^s - E^I) \times \hat{r} = (H^i + H^s - H^I) \times \hat{r} = 0 \quad (8)$$

The surface boundary conditions, satisfied as described in equation (4), are expressed in terms of the expansions of EM fields in spherical coordinates, as shown in equation (1). The expansion coefficients are obtained as a function of classical Mie Theory coefficients:

$$a_{mn}^{l} = a_n^l p_{mn}^l, \quad b_{mn}^{l} = b_n^l q_{mn}^l, \quad c_{mn}^{l} = c_n^l q_{mn}^l, \quad d_{mn}^{l} = d_n^l p_{mn}^l \quad (9)$$

Note that the incident EM field on the sphere is composed of the primary excitation field and the EM field scattered by other spheres. Therefore, to obtain the scattering coefficients of the sphere, the scattered field of the other spheres must be transformed into the new coordinate system centered at the sphere's center. This transformation is facilitated by the Translational Addition Theorem [18]. In this approach, the scattered field of an isolated sphere is treated as the incident field for the specified origin sphere, resulting in outward vector spherical wave functions (VSWF) being transformed into inward ones.

$$\bar{M}_{mn}^{(3)}(l) = \sum_{\nu=0}^{\infty} \sum_{\mu=-\nu}^{\nu} (A_{\mu\nu}^{mn}(l,j) M_{\mu\nu}^{(1)}(j) + B_{\mu\nu}^{mn} N_{\mu\nu}^{(1)}(j)) \quad (10)$$

$$\bar{N}_{mn}^{(3)}(l) = \sum_{\nu=0}^{\infty} \sum_{\mu=-\nu}^{\nu} (B_{\mu\nu}^{mn}(l,j) M_{\mu\nu}^{(1)}(j) + A_{\mu\nu}^{mn} N_{\mu\nu}^{(1)}(j)) \quad (11)$$

Equation (6) illustrates that the outward vector spherical wave functions (VSWF) can be expressed as a sum of inward VSWF using translational coefficients $A_{\mu\nu}^{mn}$ and $B_{\mu\nu}^{mn}$, where these coefficients are defined as mentioned:

$$A_{\mu\nu}^{mn} = (-1)^{\mu} i^{\nu-n} \frac{2\nu+1}{2\nu(2\nu+1)} \sum_{p=|n-\nu|}^{n+\nu} (-i)^p \times [n(n+1) + \nu(\nu+1) - p(p+1)] \times a(m,n,-\mu,\nu,p) h_p^{(1)}(kd_{j,l}) \times P_p^{m-\mu}(cos\,\theta_{j,l})\, exp[i(m-\mu)\phi_{j,l}] \quad (12)$$

$$B_{\mu\nu}^{mn} = (-1)^{\mu} i^{\nu-n} \frac{2\nu+1}{2\nu(2\nu+1)} \sum_{p=|n-\nu|}^{n+\nu} (-i)^p \times b(m.n.-\mu.\nu.p.p-1) h_p^{(1)}(kd_{j.l}) \times P_p^{m-\mu}(cos\,\theta_{j.l})\, exp[i(m-\mu)\phi_{j.l}] \quad (13)$$

As depicted in equation (7), it is evident that translational coefficients are dependent on the coordinates of the spheres, where $d_{j.l}$ represents the distance between two arbitrary spheres, $\theta_{j.l}$ and $\varphi_{j.l}$ denote the differential elevation and azimuth angles of the two mentioned spheres. To achieve the absolute value of translational coefficients Gaunt Coefficients should be calculated primarily [13].

To analyze the force exerted on small cloud drops, this section will define the Discrete Dipole Approximation (DDA) method. Given the small size parameter of the drops compared to the incident wavelength, this method comprehensively defines the scattering characteristics for the problem addressed in this paper. Particles much smaller than the wavelength can be treated as electrical dipoles. Each particle is characterized by a position vector r_l and electrical polarization α_l, enabling the direct determination of the dipole moment through dipole polarization: [19]

$$P_l = \alpha_l E_l \quad (14)$$

here E_l represents the electric field on $l-$th particle. This is followed by expression below:

$$E_l = E_{inc,l} - \sum_{k \neq l} A_{lk} P_k \quad (15)$$

$$A_{lk} = \frac{\exp(ikr_{lk})}{r_{lk}} [k^2(\hat{r}_{lk}\hat{r}_{lk} - I_3) + \quad (16)$$

$\frac{ikr_{lk}-1}{r_{lk}^2}(3\hat{r}_{lk}\hat{r}_{lk} - I_3)]$

Similar to the translational addition theorem, the scattered field by the rest of the spheres is translated onto one sphere.

3 Electromagnetic Force Exerted on a Dipole

To derive the electromagnetic force exerted on a dipole, the electrical polarization of the dipole must first be calculated. The A-1 term method provides a suitable solution to achieve electrical polarization in terms of Mie scattering coefficients [20]. In this method, polarization can be directly obtained using the first Mie scattering coefficient:

$$\alpha_l = i\frac{3a_1}{2k^3} \tag{17}$$

k represents the propagation constant in free space. By substituting equation (16) into equation (14), the dipole momentum can be calculated. The electromagnetic force exerted on a dipole due to the electromagnetic field is a function of the electrical and magnetic fields, as shown below [21]:

$$F = (p \cdot \nabla)E + p \times (\nabla \times E) + \frac{d}{dt}(p \times B) \tag{18}$$

Notably, in the DDA approach, droplets with size parameters much smaller than the incident wavelength are treated as dipoles to simplify the derivation of the exerted force. By neglecting the effect of the magnetic field, which has a smaller amplitude compared to the electrical field, a reasonable approximation is made. Equation (17) then simplifies to a simpler form:

$$F = \sum_i p_i \nabla E_i \qquad i = x.y.z \tag{19}$$

As demonstrated in equation (18), the gradient operates on a vector, resulting in a 3×3 dyadic that illustrates each component of force due to any component of the electrical field. This approach ensures that all possible conditions are considered for an anisotropic scattering medium.

4 Results and Discussion

Following the evaluation of the theoretical underpinnings concerning random scattering from spherical objects significantly smaller than the illumination wavelength in the preceding section, this section delves into three distinct cases aimed at validating the efficacy of the proposed method. For this purpose, cloud droplets are envisaged as homogeneous spheres characterized by a dielectric permittivity of $\varepsilon_r = 25{,}81 - j33{,}05$ and diameters ranging from 500 μm to 700 μm [3]. The model addresses scenarios with unfavorable conditions for rainfall, such as low wind. However, when wind is present, it can aid in cloud seeding, as the direction of droplet deviation – controlled by radiation parameters of incident wave – can be aligned to increase their speed along the wind's path, enhancing the likelihood of inducing charges on the droplets. Utilizing the discussed methodology, the exerted force is meticulously assessed across three scenarios of random distribution. Case I entails a cluster of 10 spheres, each with a diameter of d = 500 μm, while Case II comprises 10 spheres with a diameter of d = 700 μm. Case III is dedicated to evaluating a heterogeneous medium encompassing 15 spheres with diameters varying between 500 μm and 700 μm. In each instance, the EM fields are expanded using Vector Spherical Wave Functions (VSWF) as delineated in equations (1)-(3). Employing a MATLAB code, the radiation pressure, amplitude, and direction of the exerted force are discerned. The incident wave is modeled as a Gaussian plane wave propagating along the z-axis at a frequency of 28 GHz, corresponding to the realm of 5G mobile communications. Moreover, the permittivity of the cloud droplets is derived based on the operational frequency.

In the initial case, 10 homogeneous spheres exhibiting identical diameters and electrical permittivity are randomly dispersed, as depicted in Fig. 1. The salient features of the exerted force and the coordinates of the particles are succinctly outlined in Table I. The following tables, illustrate the magnitude and direction of the exerted force along each Cartesian coordinate. The first part of the table provides the droplet locations in $x.y$ and z coordinates, while the second part summarizes the exerted force in each respective direction.

In Fig. 1(a), the exerted force on each particle is depicted, with the normal vector of the force direction indicated for clarity. The force amplitude is normalized to facilitate visualization. Additionally, Fig. 1(b) presents the Radar Cross Section (RCS) of the cluster at a specific angle ($\phi = 0$) while varying the elevation angle (θ). Fig. 1(a) depict the motion direction resulting from the exerted force, based on the positions and orientations of cloud droplets. Fig. 1(b) further highlights the density distribution of droplets, with an example at φ=0 showing how droplets are dispersed. Higher RCS values indicate greater droplet density. Notably, due to the incident wave propagating along the z-axis ($\phi = 0,\ \theta = 0$), the RCS reaches its minimum value around $\theta = 90$, aligning with expectations based on the simulation setup. Further insights gleaned from Table I reveal that particles situated closer to the coordinate center interact more prominently with the incident wave, resulting in larger force amplitudes compared to particles further from the illumination angle.

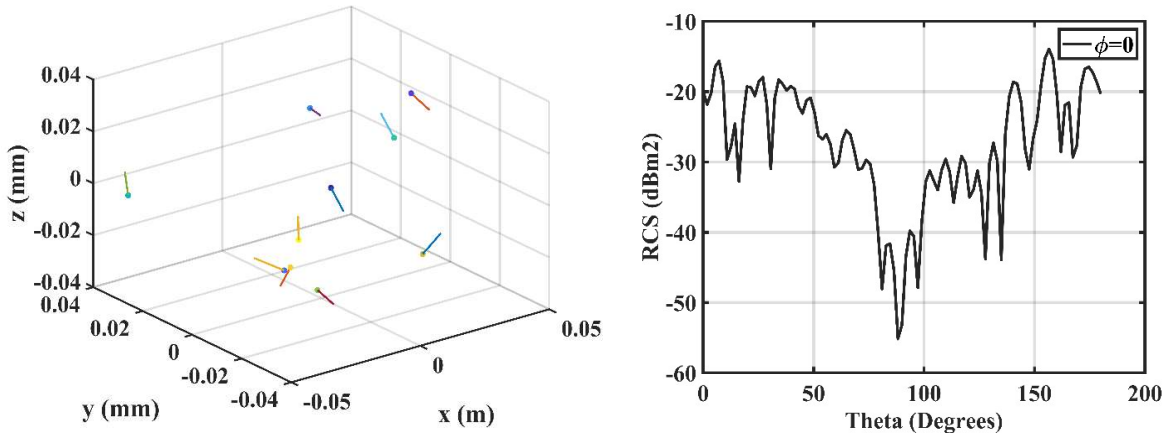

(a) (b)

Fig. 1 Results for case I. a) direction of exerted force, b) RCS of the droplet cluster on the XZ plane.

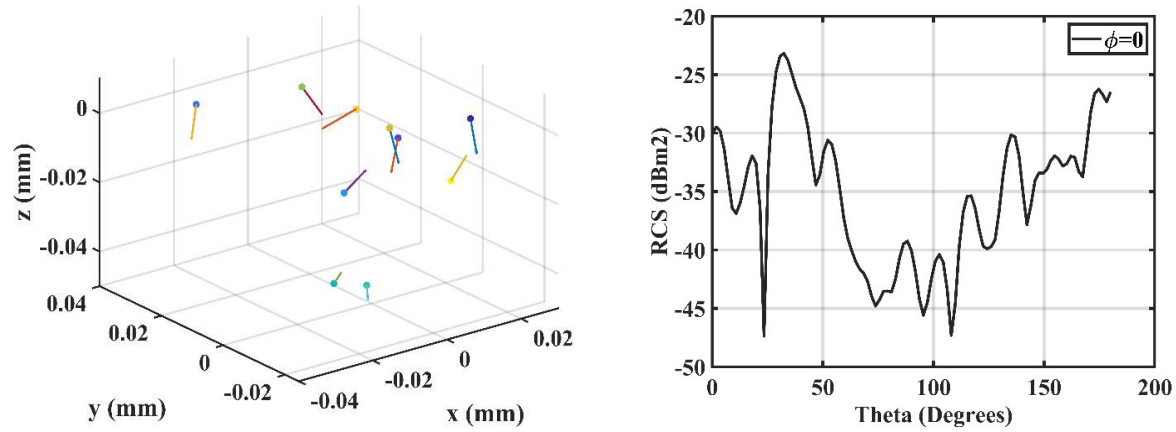

(a) (b)

Fig. 2 Results for case II. a) direction of exerted force, b) RCS of the droplet cluster on the XZ plane.

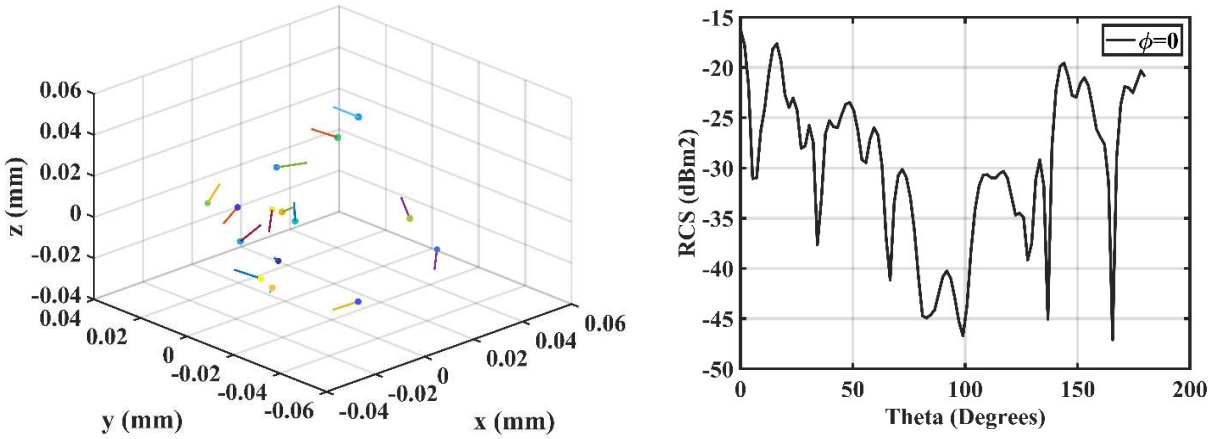

(a) (b)

Fig. 3 Results for case III. a) direction of exerted force, b) RCS of the droplet cluster on the XZ plane.

Transitioning to the second case, the diameter of the spheres is increased to 700 μm to assess a distinct cluster and simulation configuration. Maintaining the same permittivity as the previous case, homogeneous spheres characterized by $\varepsilon_r = 25{,}81 - j33{,}05$ are considered. Fig. 2(a) illustrates the force direction and particle distribution, while Table II provides detailed information regarding particle coordinates and the exerted force on each particle.

In the third case, a novel simulation setup is employed, featuring droplets with diameters ranging from 500 μm to 700 μm. Here, 15 spheres are positioned arbitrarily, and the force amplitude as well as direction are computed using the established methodology. Similarly, Fig. 3(a-b) visually represents the particle distribution and the Radar Cross Section (RCS) for this scenario. Furthermore, Table III succinctly summarizes the particle coordinates and details pertaining to the exerted force. This case serves to investigate the impact of heterogeneity and varying droplet sizes on the characteristics of the exerted force, consequently influencing motion direction.

Table I The coordinates and components of exerted force for the case I.

Particle no.	coordinates			Exerted Force		
	x (mm)	y (mm)	z (mm)	Fx (μN)	Fy (μN)	Fz (μN)
1	0.9	-2.9	3.6	-4.31	-16	-12
2	34.8	0	29.2	3.1	-0.09	-0.4
3	-8.5	6.2	-29.7	-1.18	1.21	0.73
4	2.3	6.9	29.5	-1.22	-2.64	0.64
5	-44.1	32	-2.6	0	0	0.05
6	7.1	-22	29.9	0.1	0.5	0.44
7	0.8	2.3	-38.1	-0.6	-2.28	-0.17
8	39.3	0	-34	0.17	-0.7	0.25
9	-39.4	-28.7	-3.9	-0.01	0.04	-0.11
10	-29	-21.1	0.3	-0.01	0	0.18

Upon evaluating Case III, it becomes apparent that the force exerted on each particle is contingent upon both its size and location within the medium. Those particles situated closer to the illumination angle experience a greater force, while smaller particles are subjected to comparatively larger forces. The velocity of the particles must be considered in light of various factors such as initial velocity and wind direction.

The primary purpose of using EM waves in this paper is to induce controlled motion of droplets, bringing them into coincidence and contact, which results in the induction of electrical charge on each droplet. It is assumed that the droplets initially carry no charge, and conditions are set to be unfavorable for rainfall.

Table II The coordinates and components of exerted force for the case II.

Particle no.	coordinates			Exerted Force		
	x (mm)	y (mm)	z (mm)	Fx (μN)	Fy (μN)	Fz (μN)
1	26.7	0	-4.6	-0.01	-0.29	-0.07
2	7.2	0	-4.3	-0.79	-0.54	-1.37
3	-29.4	21.4	7.3	-0.044	-0.036	-.076
4	4.7	14.5	-25.6	0.24	0.081	0.084
5	-25.7	-18.7	-28.5	-0.069	0.142	0.156
6	-3.2	-2.4	-42.7	-0.12	-0.15	0.012
7	12	36.9	-6.7	0.047	-0.032	-.107
8	1.4	-4.2	2.1	-1.16	-4.5	-8.74
9	-2.5	1.9	6.2	-2.9	0.37	-1.27
10	6	-18.5	-8.5	-0.107	-0.28	0.68

Table III The coordinates and components of exerted force for the case III.

Particle no.	coordinates			Exerted Force		
	x (mm)	y (mm)	z (mm)	Fx (μN)	Fy (μN)	Fz (μN)
1	-0.9	-6.5	-13.6	-7.11	-5.3	7.39
2	-11.5	8.3	6.9	-0.22	0.26	-0.67
3	7.6	-23.4	-32.9	-0.17	0.26	-0.2
4	15.8	-48.6	0.4	-0.02	0	-0.12
5	1.8	5.6	21.9	0.28	-0.23	0.07
6	29.9	0	36.9	-0.1	0.08	0.1
7	9.5	29.1	-28	0.04	-0.01	0.04
8	1	-3.2	0	-0.92	-0.29	14.89
9	21.5	0	30.5	-0.18	0.12	0.13
10	-18.7	13.6	9.7	1.35	-0.54	3.18
11	50.9	0	-21.5	0.01	0.03	0.03
12	0.6	1.9	2.3	-13.95	-52.99	48.21
13	-16.7	-12.1	-20.9	0.51	0.68	-0.82
14	-17	-12.3	17.3	-0.59	-0.45	-0.89
15	-5.8	4.2	-28.4	-0.19	0.59	0.12

The polarization in a dielectric material can be related to an equivalent surface charge density, as:

$$\sigma_{eq} = p/V \tag{20}$$

where p is the dipole moment and V is the droplet volume, respectively. The equivalent induced charge on the droplet can then be estimated by multiplying this surface charge density by the droplet's surface area:

$$q_{ind} = \sigma_{eq} A = \sigma_{eq} \pi R^2 \tag{21}$$

This q_{ind} gives an estimate of the total induced charge due to the polarization effects in the droplet under the external electric field.

Assuming cloud droplets move at a constant velocity V_0 in a primary direction, the exerted force will induce motion in the direction of the force, with acceleration stemming from the force itself:

$$F = ma \quad (22)$$

The resultant velocity of the droplets post-application of the Lorentz force can be determined by the equation:

$$V - V_0 = at \quad (23)$$

Intentional deviation of the particles can be achieved through strategic choices regarding incident wave characteristics, such as illumination angle or wave polarization. Additionally, the operational frequency can influence the magnitude of force exerted on the particles. By directing droplets from less dense to denser mediums, the likelihood of coincidental collisions leading to fertilization and subsequent precipitation can be augmented.

5 Conclusion

In conclusion, this paper explored the application of electromagnetic (EM) waves in addressing environmental challenges, particularly drought and precipitation. By treating the cloud medium as a heterogeneous entity comprising spherical droplets, EM scattering was examined utilizing a linearly polarized incident plane wave. Through computation of the local electric field on each particle and accounting for multiple scattering, the magnitude and direction of the Lorentz force on each droplet were determined using Generalized Mie Theory (GMT) and Discrete Dipole Approximation. The deliberate deviation and stirring of droplets to enhance coincidental collisions were achieved through varying incident wave characteristics such as frequency, polarization, and illumination angle. The droplet density significantly impacts the RCS values, with a maximum of -15dBm^2 observed for varying droplet distributions. As the RCS increases and particles are closer to the excitation wave origin, the exerted force varies notably, ranging from 0.1217 to 72.98 (μN). This variation highlights the influence of both particle proximity and size on force exerted in such distributions. The efficacy of the hybrid algorithm in calculating the Lorentz force on each cloud droplet was validated through the examination of several cases featuring different droplet diameters and electrical properties.

References

[1] F. Norouzian, E. Marchetti, M. Gashinova, E. Hoare, C. Constantinou, P. Gardner and M. Cherniakov, “Rain attenuation at millimeter wave and low-THz frequencies,” IEEE Transactions on Antennas and Propagation, vol. 68, no. 1, pp. 421-431, Sep. 2019.

[2] I. Shayea, T. Abd. Rahman, M. Hadri Azmi and A. Arsad, “Rain attenuation of millimetre wave above 10 GHz for terrestrial links in tropical regions,” Transactions on emerging telecommunications technologies, vol. 29, no. 8, p. 3450, Aug. 2018.

[3] M. Bahrami and J. Rashed-Mohassel, “An exact solution of coherent wave propagation in rain medium with realistic raindrop shapes,” Progress in Electromagnetics Research, vol. 79, pp. 107-118, Jul. 2008.

[4] B. Yektakhah and K. Sarabandi, “Physics-Based Coherent Modeling of Long-Range Millimeter-Wave Propagation and Scattering in Rain,” IEEE Open Journal of Antennas and Propagation, Jun 2023.

[5] Q.-f. Dong, Y.-L. Li, J.-d. Xu, H. Zhang, and M.-j. Wang, "Effect of sand and dust storms on microwave propagation," IEEE Transactions on Antennas and Propagation, vol. 61, pp. 910-916, 2013.

[6] A. N. Moqadam and R. Kazemi, "High-Resolution Imaging of Narrow Bone Fractures with a Novel Microwave Transceiver Sensor Utilizing Dual-Polarized RIS and SRR Array Antennas," in IEEE Sensors Journal, vol. 23, no. 24, pp. 30335-30344, 15 Dec.15, 2023, doi: 10.1109/JSEN.2023.3328240.

[7] L. Tsang, J. A. Kong, and K.-H. Ding, Scattering of Electromagnetic Waves, Theories and Applications vol. 27: John Wiley & Sons, 2004.

[8] A. Ishimaru, Electromagnetic wave propagation, radiation, and scattering: Prentice-Hall, 1991.

[9] Y.-l. Xu, "Electromagnetic scattering by an aggregate of spheres," Applied optics, vol. 34, pp. 4573-4588, 1995.

[10] Y.-l. Xu, "Scattering Mueller matrix of an ensemble of variously shaped small particles," JOSA A, vol. 20, pp. 2093-2105, 2003.

[11] M. I. Mishchenko, L. D. Travis, and D. W. Mackowski, "T-matrix computations of light scattering by nonspherical particles: a review," Journal of Quantitative Spectroscopy and Radiative Transfer, vol. 55, pp. 535-575, 1996.

[12] B. T. Draine and P. J. Flatau, "Discrete-dipole approximation for scattering calculations," JOSA A, vol. 11, pp. 1491-1499, 1994.

[13] A. N. Moqadam, A. Pourziad and S. Nikmehr, “Motion of small spherical particles in an arbitrary oriented cluster due to the microwave propagation,” Progress in Electromagnetics Research B, vol. 76, pp. 97-110, 2017.

[14] A. N. Moqadam, A. Pourziad and S. Nikmehr, “Radiation Forces on a Cluster of Spherical Nanoparticles in Visible Light Spectrum,” Progress in Electromagnetics Research C, vol. 75, pp. 75-99, 2017.

[15] M. Kokkonen, H. Juttula, A. Mäkynen, S.

Myllymäki, and H. Jantunen, "The effect of drop shape, sensing volume and raindrop size statistics to the scattered field on 300 GHz," IEEE Access, vol. 9, pp. 101381-101389, 2021.
[16] Y. Averyanova, A. Rudiakova, and F. Yanovsky, "Drop deformation estimate with multi-polarization radar, " International Journal of Microwave and Wireless Technologies, vol. 12, no. 9, pp. 870-877, 2020.
[17] A. and Md. Rafiqul Islam,"Path loss models for outdoor environment—with a focus on rain attenuation impact on short-range millimeter-wave links," e-Prime-Advances in Electrical Engineering, Electronics and Energy, vol. 3 p. 100106, 2023.
[18] T. J. Dufva, J. Sarvas, and J. C.-E. Sten, "Unified derivation of the translational addition theorems for the spherical scalar and vector wave functions," Progress in Electromagnetics Research B, vol. 4, pp. 79-99, 2008.
[19] B. T. Draine and P. J. Flatau, "Discrete-dipole approximation for scattering calculations," JOSA A, vol. 11, pp. 1491-1499, 1994.
[20] H. Okamoto, "Light scattering by clusters: the al-term method," Optical Review, vol. 2, pp. 407-412, 1995.
[21] L. Novotny and B. Hecht, “Principles of nano-optics,” Cambridge university press, 2012.

Aslan Nouri Moqadam received the B.S. degree in electrical engineering from the University of Tabriz, Tabriz, Iran, in 2009, followed by the M.S. and Ph.D. degrees from the same university in 2016 and 2023, respectively. Since 2010 he has been a Research collaborator with the UWB laboratory. His research interests include electromagnetic propagation and design of antennas and microwave components for biomedical applications.

Seyed Hosein Mousavi received the B.S. degree in electrical engineering from the Shahid Sattari University of Aeronautical Engineering, Tehran, Iran, in 2005, followed by the M.S. degree from the Malek-e-Ashtar University, Tehran, Iran, in 2010. After that, he received Ph.D. degree from the University of Tabriz, Tabriz, Iran, in 2022. His research interests include wireless communication systems and signal processing and electromagnetic propagation.